Available online at www.sciencedirect.com
ScienceDirect
Dyes and Pigments 79 (2008) 7–13
DYES and PIGMENTS
www.elsevier.com/locate/dyepig

The crystal structure and optical properties of 1-methyl-4-[2-(4-hydroxyphenyl)ethenyl]pyridinium dihydrogenphosphate: New aspects on crystallographic disorder and its effect on polarized solid-state IR spectra

Tsonko Kolev [a], Bojidarka B. Koleva [b,*], Michael Spiteller [a], Heike Mayer-Figge [b], William S. Sheldrick [b]

[a] *Institut für Umweltforschung, Universität Dortmund, Otto-Hahn-Strasse 6, 44221 Dortmund, Germany*
[b] *Lehrstuhl für Analytische Chemie, Ruhr-Universität Bochum, Universitätsstraße 150, 44780 Bochum, Germany*

Received 10 October 2007; received in revised form 17 December 2007; accepted 19 December 2007
Available online 3 January 2008

Abstract

The novel, 1-methyl-4-[2-(4-hydroxyphenyl)ethenyl]pyridinium dihydrogenphosphate salt was synthesized and its structure and properties elucidated spectroscopically, thermally and structurally, using single crystal X-ray diffraction, linear-polarized solid-state IR spectroscopy (IR-LD), UV–vis spectroscopy, TGA, DSC, DTA and MS. The compound crystallizes in the monoclinic $P2_1/c$ space group and exhibits a pseudo layer structure with molecules linked by strong OH···O–P intermolecular hydrogen bonds of length 2.593 Å. The dihydrogenphosphate anions themselves form infinite chains through strong OH···O–P intermolecular hydrogen bonds of lengths 2.636 and 2.658 Å. The crystallographic disorder of these systems and its effect on IR-LD spectra in the solid state are discussed. Solutions of different polarity show a significant CT band shift of up to 70 nm, corresponding to a molecular first hyperpolarizability value.

Keywords: 1-Methyl-4-[2-(4-hydroxyphenyl)ethenyl]pyridinium dihydrogenphosphate; Single crystal X-ray data; Solid-state linear-polarized IR spectroscopy; UV–vis; MS; TGV

1. Introduction

Interest in pyridinium salts during recent 30 years has been due to many of the derivatives possessing large second-order molecular hyperpolarizabilities. Studies of the second harmonic generation (SHG) from powders and Langmuir–Blodgett films of these merocyanine dyes have attracted much attention due to their application in various areas of nonlinear optics. Second-order nonlinear optical properties of these materials are very sensitive to the symmetry of the structure [1–4]. It has been found that the variation of the counterion in organic salts provides a simple and highly successful approach to create materials with larger χ values. This methodology has been also supported by the observed crystal structure and properties of DAST [1].

We now present a spectroscopic and structural elucidation of the novel salt 1-methyl-4-[2-(4-hydroxyphenyl)ethenyl]pyridinium hydrogenphosphate (Scheme 1) as part of our systematic study of new materials with potential NLO application [5–8]. The relationship between structural and spectroscopic properties is elucidated using single crystal X-ray diffraction, UV–vis and fluorescence methods, polarized linear-dichroic infrared (IR-LD) spectroscopy of oriented colloid suspensions in a nematic liquid crystal, mass spectrometry, TGV and DSC methods. The usual observed crystallographic disorder and the effect of the aromatic–quinoide equilibrium of these compounds on the optical spectroscopic characteristics are discussed.

* Corresponding author. Tel.: +49 234 32 24190.
E-mail address: bkoleva@chem.uni-sofia.bg (B.B. Koleva).

0143-7208/$ - see front matter © 2007 Elsevier Ltd. All rights reserved.
doi:10.1016/j.dyepig.2007.12.007

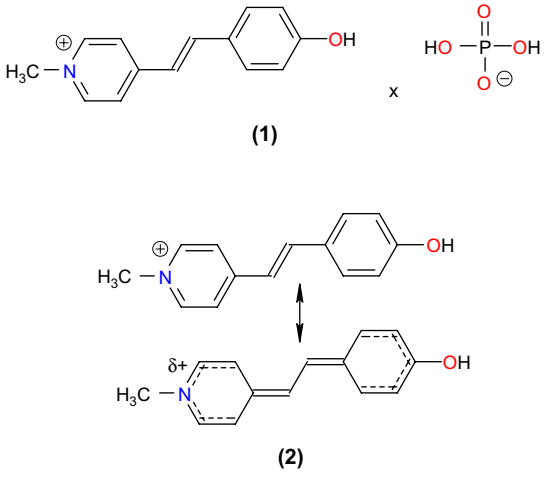

Scheme 1. Chemical diagram of 1-methyl-4-[2-(4-hydroxyphenyl)ethenyl]pyridinium hydrogenphosphate (1) and scheme of the aromatic–quinoide transition (2).

2. Experimental

2.1. Materials

The starting compounds for the synthesis of 1-methyl-4-[2-(4-hydroxyphenyl)ethenyl] pyridinium iodide, 1,4-dimethylpyridinium iodide and 4-hydroxybenzaldehyde were Merck (Germany) products. The reaction scheme (Scheme 2) for obtaining 1-methyl-4-[2-(4-hydroxyphenyl)ethenyl] pyridinium iodide is as follows: 2.35 g (10 mmol) 1,4-dimethylpyridinium iodide is mixed with 1.22 g (10 mmol) 4-hydroxybenzaldehyde in 50 ml toluene. Acetic acid (5 ml) and 0.77 g (10 mmol) ammonium acetate are also added to the reaction mixture. Thus obtained suspension is stirred for 24 h at room temperature. Then 0.5 ml concentrated HI and 10 ml ethanol are added and the obtained reaction mixture left to stand for 16 h at room temperature. The orange precipitate received is filtered off, washed with C_2H_5OH and dried on P_2O_5 at 298 K. Yield 73%. M.p. 274–275 °C and TLC factor of $R_f = 0.16$ (Al_2O_3/CH_3OH). Found: C, 49.6; H, 4.2; N, 4.16; [$C_{14}H_{14}NOI$] calcd.: C, 49.0; H, 4.2; N, 4.16%. 1-Methyl-4-[2-(4-oxocyclohexadienilydene)ethylidene]-1,4-dihydropyridine is then obtained in the following way: 10.0 mg of iodide salt is dissolved in 10.00 mmol ethanol and then 5 ml 1.0 M KOH is added. The obtained lilac solution is heated for 2 h at a temperature of 70 °C, and then is kept at 4 °C for 16 h. The obtained violet precipitate is filtered off, dried on P_2O_3 at 298 K. Yield 98%. M.p. 222–224 °C and $R_f = 0.45$ (cellulose/CH_3OH). Found: C, 75.6; H, 6.2; N, 6.7; [$C_{14}H_{13}NO$] calcd.: C, 75.5; H, 6.2; N, 6.7%. Finally, 1-methyl-4-[2-(4-hydroxyphenyl)ethenyl]pyridinium dihydrogenphosphate is obtained by mixing equimolar amounts of the quinoide derivative and H_3PO_3 in 20 ml solvent mixture of water:methanol 1:1. The obtained mixture is stirred for 10 h at 40 °C. The obtained solution is cooled at 4 °C for 10 h. Finally the obtained orange precipitate is filtered off, washed with methanol and dried on P_2O_5 at 298 K. Yield 61%. Found: C, 54.4; H, 5.2; N, 4.4; [$C_{14}H_{16}NO_5P$] calcd.: C, 54.4; H, 5.2; N, 4.5%.

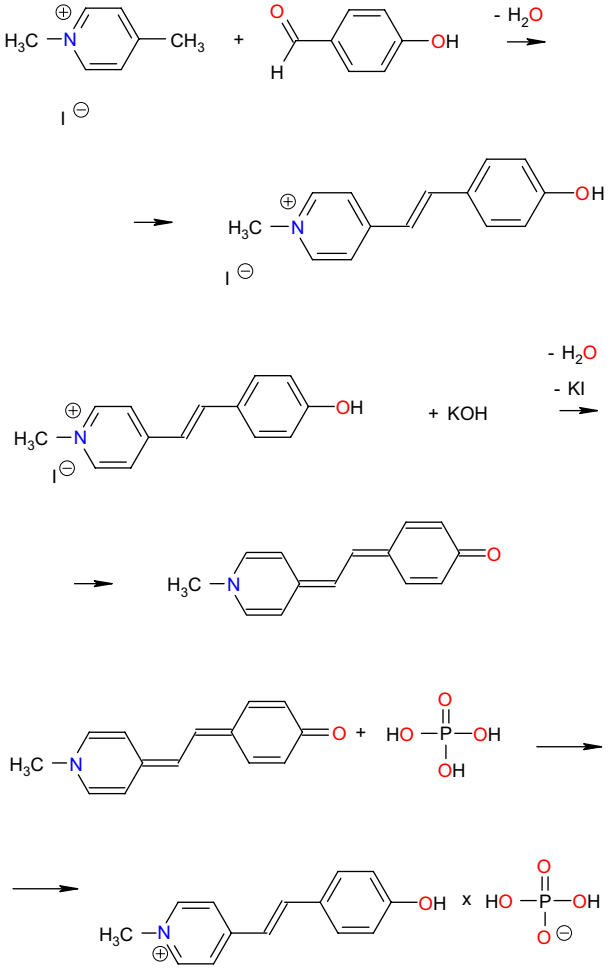

Scheme 2. Reaction scheme.

TGV and DSC analyses in the range 300–500 K indicated that no solvent was included in any of the obtained compounds.

The most intensive signal in the mass spectrum of the title compound is that of the peak at *m/z* 213.31, corresponding to the singly charged cation $[C_{12}H_{15}NO]^+$ with a molecular weight of 213.27.

2.2. Methods

2.2.1. X-ray diffraction

The *X-ray diffraction* intensities were measured in the ω scan mode on a Siemens P4 diffractometer equipped with Mo Kα radiation ($\lambda = 0.71073$ Å $\theta_{max} = 25°$). The single crystal X-ray diffraction data and the structure were solved by direct methods and refined against F_0^2 [9,10]. An ORTEP plot illustrates the anion and cation structures at the 50% probability level. Relevant crystallographic structure data and refinement details are presented in Table 1, selected bond distances and angles in Table 2. The hydrogen atoms were constrained to calculated positions and refined using riding models in all cases. As there are no atom types heavier than oxygen in the structure, the absolute structure could not be determined with Mo Kα radiation.

Table 1
Crystal data, data collection and refinement conditions for $C_6H_7N_3O_2$

Empirical formula	$C_{14}H_{16}NO_5P$
Formula weight	309.25
Temperature	173(2)
Wavelength	0.71073 Å
Crystal system, space group	Monoclinic, $P21/c$
Unit cell dimensions	$a = 7.581(3)$ Å, $b = 16.191(7)$ Å, $c = 11.532(5)$ Å, $\beta = 91.42(3)^\circ$
Volume	1415.0(10) Å^3
Z	4
Calculated density	1.452
Absorption coefficient	0.216
$F(000)$	648
Crystal size	0.28 × 0.31 × 0.48 mm
θ Range for data collection	2.98–24.97°
Limiting indices	$-8 \le h \le 8$, $-19 \le k \le 14$, $-13 \le l \le 10$
Absorption correction	0.11319
Refinement method	Full-matrix least-squares on F^2
Goodness-of-fit on F^2	1.084
Final R indices $[I > 2\sigma(I)]$	$R1 = 0.0585$, $wR2 = 0.1605$
R indices (all data)	$R1 = 0.0662$, $wR2 = 0.1693$

2.2.2. Conventional and polarized IR spectroscopy

The *IR spectra* were measured on a Thermo Nicolet OMNIC FTIR spectrometer (4000–400 cm^{-1}, 2 cm^{-1} resolution, 200 scans) equipped with a Specac wire-grid polarizer. Non-polarized solid-state IR spectra were recorded using the KBr disk technique. The *oriented samples* were obtained as a suspension in a nematic liquid crystal (MLC 6815, Merck) with the presence of an isolated nitrile stretching IR band at about 2245 cm^{-1} additionally serving as an orientation indicator. The theoretical approach, experimental technique for preparing the samples, procedures for polarized IR spectra interpretation and the validation of this new linear-dichroic infrared (IR-LD) orientation solid-state method for accuracy, precision and the influence of the liquid crystal medium on peak positions and integral absorbances of the guest molecule bands have been presented previously [11–13]. The nature and balance of the forces in the nematic liquid crystal suspension system, the mathematical model for their clearance, morphology of the suspended particles and the influence of the space system types on the degree of orientation (i.e. the ordering parameter) have been investigated [12] using five liquid crystals and fifteen compounds. The applicability of the last approach to experimental IR spectroscopic band assignment as well as in obtaining stereo-structural information has been demonstrated in a series of organic systems and coordination complexes of heterocyclic ligands, Cu(II) complexes, polymorphs, codeine derivatives, Au(III) peptide complexes and their hydrochlorides and hydrogensquarates [14–17]. The theory of IR-LD spectroscopy and the employed polarized IR spectra interpretation difference-reduction procedure are given in Refs. [18–21].

2.2.3. Mass spectral data

The FAB mass spectra were recorded on a Fisons VG autospect instrument employing 3-nitrobenzylalcohol as the matrix.

2.2.4. UV spectra

UV spectra were recorded on Tecan Safire Absorbance/Fluorescence XFluor 4 V 4.40 spectrophotometer operating between 190 and 900 nm, using solvents water, methanol, dichloromethane, tetrahydrofuran, acetonitrile, acetone, 2-propanol and ethylacetate (all Uvasol, Merck products) in concentration of 2.5×10^{-5} M, using 0.0921 cm quartz cells.

2.2.5. Quantum chemical calculations

They were performed with GAUSSIAN 98 program package [22]. The output files are visualized by means of the ChemCraft program [23].

The geometry of the cation was optimized at two levels of theory: second-order Moller–Pleset perturbation theory

Table 2
Selected bond lengths [Å] and angles [°] for $C_6H_7N_3O_2$

N1 C2 1.343(4)	C4′ C7′ 1.56(2)	C3 C4 C5 119.5(11)	C2 N1 C6 120.9(3)
N1 C6 1.346(4)	C7′ C8′ 1.498(8)	C3 C4 C7 123.2(7)	C2 N1 C1 119.1(3)
N1 C1 1.481(4)	C8′ C9′ 1.53(2)	C5 C4 C7 116.8(7)	C6 N1 C1 120.0(3)
C2 C3 1.360(4)	C9′ C14 1.418(15)	C8 C7 C4 127.8(5)	C2 C3 C4 119.4(6)
C3 C4 1.373(10)	C9′ C10 1.422(14)	C7 C8 C9 125.0(5)	C2 C3 C4′ 122.4(10)
C3 C4′ 1.440(16)	C10 C11 1.369(4)	C10 C9 C14 116.5(9)	C4 C3 C4′ 13.9(18)
C5 C4 1.376(10)	C11 C12 1.391(4)	C10 C9 C8 116.1(6)	C4 C5 C6 118.9(6)
C5 C6 1.375(6)	C12 O1 1.361(4)	C14 C9 C8 126.9(7)	C4 C5 C4′ 13.8(18)
C5 C4′ 1.444(16)	C12 C13 1.400(4)	C3 C4′ C5 110.8(16)	C6 C5 C4′ 122.0(10)
C4 C7 1.442(16)	C13 C14 1.369(4)	C3 C4′ C7′ 111.9(9)	N1 C6 C5 120.0(3)
C7 C8 1.359(6)	P1 O4′ 1.497(2)	C5 C4′ C7′ 137.3(12)	C9′ C8′ C7′ 123.1(8)
C8 C9 1.462(14)	P1 O1′ 1.513(2)	C8′ C7′ C4′ 114.7(8)	C14 C9′ C10 114.3(16)
C9 C10 1.400(9)	P1 O2′ 1.575(2)	C11 C10 C9′ 120.7(9)	C14 C9′ C8′ 117.8(9)
C9 C14 1.406(9)	P1 O3′ 1.576(2)	C9 C10 C9′ 18.2(7)	C10 C9′ C8′ 127.9(11)
		C10 C11 C12 119.2(3)	C11 C10 C9 122.4(6)
		O1 C12 C11 122.4(3)	O1 C12 C13 118.1(3)
		C13 C14 C9′ 119.4(9)	C11 C12 C13 119.4(3)
		C9 C14 C9′ 18.2(7)	C13 C14 C9 121.0(5)
		O4′ P1 O1′ 115.33(12)	O4′ P1 O3′ 111.66(11)
		O4′ P1 O2′ 106.75(13)	O1′ P1 O3′ 105.92(11)
		O1′ P1 O2′ 110.30(12)	O2′ P1 O3′ 106.60(12)

(MP2) and density functional theory (DFT) using the 6-311++G** basis set. The DFT method employed is B3LYP, which combines Backe's three-parameter non-local exchange function with the correlation function of Lee, Yang and Parr. Molecular geometries of the studied species were fully optimized by the force gradient method using Bernys' algorithm. For every structure the stationary points found on the molecule potential energy hypersurfaces were characterized using standard analytical harmonic vibrational analysis. The absence of the imaginary frequencies, as well as of negative eigenvalues of the second-derivative matrix, confirmed that the stationary points correspond to minima of the potential energy hypersurfaces. The calculation of vibrational frequencies and infrared intensities were checked to establish which kind of performed calculations agree best with the experimental data. The DFT method provides more accurate vibrational data, as far as the calculated standard deviations corresponding to the groups which did not interact intra- or intermolecularly of respectively 8 cm^{-1} (B3LYP) and 24 cm^{-1} (MP2) are concerned. So, the B3LYP/6-311++G** data are presented for above discussed modes, where a modification of the results using the empirical scaling factor 0.9614 is made to achieve better correspondence between the experimental and theoretical values. The UV spectra of **1** in gas phase and in ethanol, water, acetonitrile and methanol solutions are obtained by CIS/6-311++G** and TDDFT calculations.

2.2.6. Thermal analysis

The thermal analyses were realized at 25–300 °C by Differential Scanning Calorimeter Perkin–Elmer DSC-7, Differential Thermal Analyzer DTA/TG (Seiko Instrument, model TG/DTA 300). The experiments were carried out with scanning rate of 10 K/min under argon atmosphere.

2.2.7. Elemental analysis

The elemental analysis was carried out according to the standard procedures for C and H (as CO_2 and H_2O) and N (by the Dumas method).

3. Results and discussion

3.1. Crystal and electronic structure

1-Methyl-4-[2-(4-hydroxyphenyl)ethenyl]pyridinium hydrogenphosphate crystallizes in the monoclinic $P2_1/c$ space group (Fig. 1). The molecules are joined into infinite parallel pseudo layers (Fig. 2) by strong intermolecular OH···O–P hydrogen bonds of length 2.593 Å and OH···O angle of 166.45°. The dihydrogenphosphate anions form infinite chains by strong (P)OH···O(P) bonds with lengths of 2.636 and 2.658 Å (Fig. 2). The molecule of the dye is absolutely flat with a deviation of total planarity of 0.2°. The bond lengths and angles of the benzene ring and the pyridine fragment are similar to aromatic character. The corresponding values of geometry parameters (Table 2) correlated with those of other merocyanine dye derivatives as *trans*-4-(4′-(*N*,

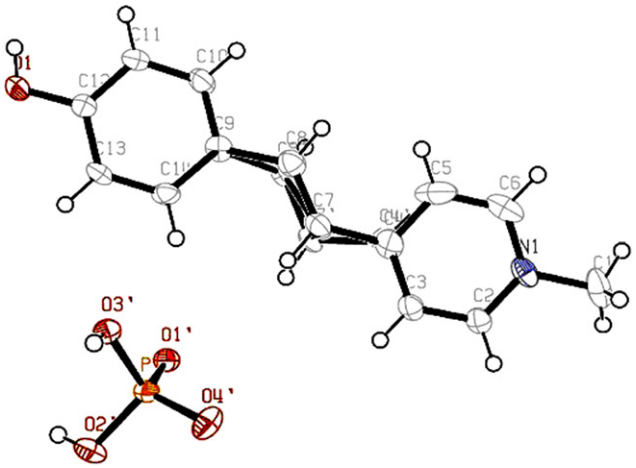

Fig. 1. The molecular structure of 1-methyl-4-[2-(4-hydroxyphenyl)ethenyl]-pyridinium hydrogenphosphate, showing the atom-labelling scheme. Displacement ellipsoids are drawn at the 50% probability level.

N-diphenylamino)styryl)-*N*′-methylpyridinium iodide, 4-[4-methoxy-α-styryl]-*N*-isopentylpyridinium bromide sesquihydrate as *est* [24–27]. Similar to other crystallographic studies of this class of organic compounds crystallographic disorder of C7 and C8 in the dye leads to the observation of either a central double (C7–C8) or single bond (C7′–C8′) due to a deviation of the high π-conjugated system. Although deviation of the conjugacy must presumably be intrinsic as in Refs. [28,29], the presence of a static disorder cannot be ruled out (Schemes 1 and 3). The multitemperature investigations of this phenomenon [30,31] led to the conclusions that the shrinkage of the C=C bond is an artifact of torsion vibration of the C–phenyl bond. If the amplitude of the torsion vibration is large enough it gives rise to conformational interconversion and hence to dynamic disorder in the crystal. In our case we could present the results schematically (Scheme 3), which is in accordance with Ref. [31]. The dynamic disorder cannot usually be resolved in a routine experiment.

3.2. IR spectra

The observed significant degree of macro-orientation in the polarized IR spectrum of sample facilitates an adequate interpretation of the polarized IR data and results from the presence of a pseudo layer structure, which adopts a macro-orientation in the solid phase toward the orientation director (**n**) of the liquid crystal. The detailed IR-LD spectroscopic analysis is supported by the theoretical vibrational analysis at B3LYP/6-311++G**. The non-polarized IR spectrum shows a relatively intensive band at 3224 cm^{-1} corresponding to stretching ν_{OH} vibration of the hydrogen bonded OH-group in merocyanine dyes, thus correlating with the obtained crystallographic data. The broad absorption band between 3000 and 1800 cm^{-1} is attributed to ν_{OH} of dihydrogenphosphate anions. Also corresponding to these species are the stretching vibration bands at 1270 cm^{-1} ($\nu_{P=O}$) and 1170 cm^{-1} (ν_{P-O}). Aromatic i.p. modes of benzene and pyridine rings at

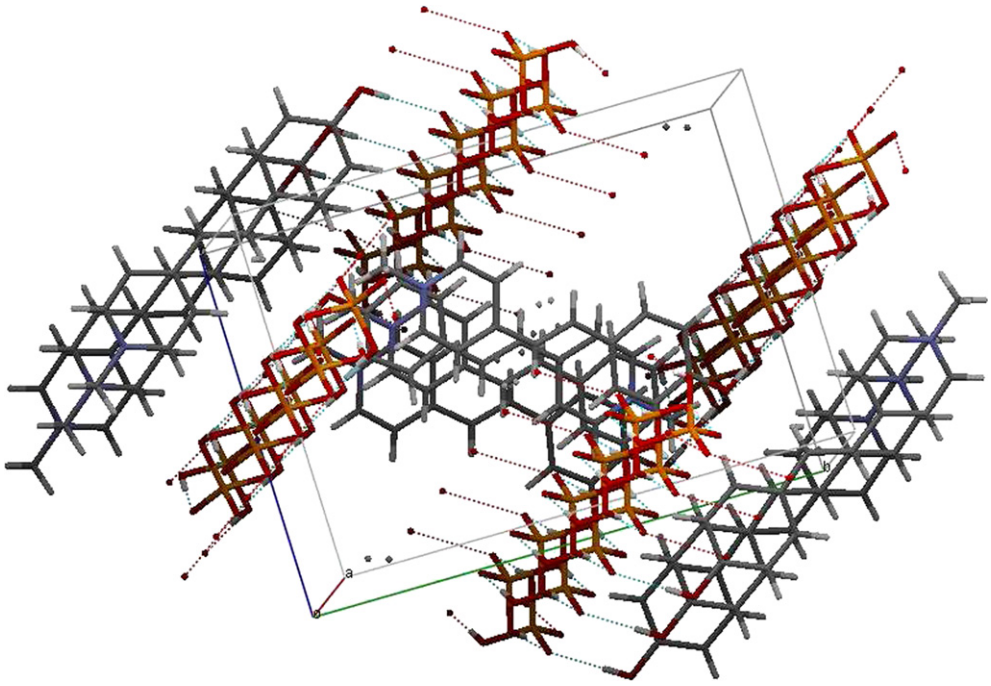

Fig. 2. Linkage of the molecules of 1-methyl-4-[2-(4-hydroxyphenyl)ethenyl]pyridinium hydrogenphosphate into infinite layers.

1623 cm^{-1} (**8a**$_{(py)}$) and 1598 cm^{-1} (**8a**$_{(Ph)}$) are observed in the range 1700–1600 cm^{-1} as broad bands. The band at 1338 cm^{-1} corresponds to the symmetric bonding vibration of N–CH_3 group ($\delta^{s}_{CH_3}$) and the obtained value is similar to those of other merocyanine dyes studied with a difference of ±4 cm^{-1}. The absorption bands belonging to out-of-plane (o.p.) bending vibrations $\nu_{C=C}$, 11-ν_{CH} benzene and o.p. mode of pyridine rings are observed at 966 cm^{-1}, 836 cm^{-1} and 765 cm^{-1}. However, both in the first and discuss IR regions the characteristics of quinoide form of the compounds studied are fined. Low intensive bands at 1550 cm^{-1}, 941 cm^{-1} and 798 cm^{-1} could be assigned to $\nu_{C=C}$ stretch and out-of-plane ν_{CH} modes of tri- and *cis*-disubstituted double bonds. The values are typical for quinoide form of these merocyanine dyes. Spectroscopic support for the X-ray structure is obtained by application of the reducing difference procedure to polarized IR spectra, where the elimination of the bands at 1623 cm^{-1}, 1598 cm^{-1} and 1338 cm^{-1} in same dichroic ratio is possible when the corresponding transition moments are co-linear oriented (see Scheme 3). On the other hand, the disappearance of the bands at 966 cm^{-1}, 836 cm^{-1} and 765 cm^{-1} (Scheme 1 and Fig. 3(2)) indicates the co-planar disposition of the rings and double bonds (Schemes 1 and 3) and is in good agreement with the crystallographic structure. The elimination of the bands at 941 cm^{-1} and 798 cm^{-1} in equal dichroic ratio (Fig. 3(3)) confirms the above stated comments.

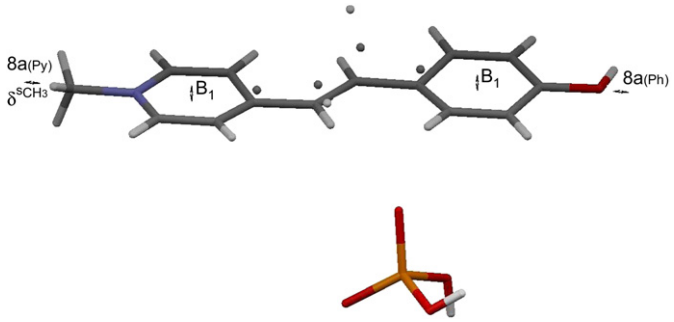

Scheme 3. Visualization of selected transition moment directions.

3.3. UV spectra

The possible redistribution of the electronic density in these compounds as typical push–pull systems depends on the solvent polarity. When the electron transition is connected with intramolecular charge transfer (CT) this leads to a significant difference between the dipole moment in the ground and excited states, that determines their significant solvatochromism, or NLO properties in solution. Depending on the solvent polarity the CT band in 1-methyl-4-[2-(4-hydroxyphenyl)ethenyl]-pyridinium hydrogenphosphate exhibits a bathochromic shift of up to 66 nm (Fig. 4) on going from H_2O to 1,2-dichloromethane. The obtained negative solvatochromic effect in these compounds has been explained by both intra and intermolecular charge transfers. In an ethanol:water solvent mixture (1:1) two bands are registered at 386 nm and 492 nm. The observation of two bands in acetonitrile, as well as the spectral changes and the well-defined isobestic points at 450 nm provide good evidence for an equilibrium between monomeric and dimeric species [15,16,18,19,23–26]. It is noteworthy that in addition to the very intense hypsochromically shifted absorption band for the *H*-dimer (Scheme 4), a weak band appears at longer wavelength which can be ascribed to the forbidden transition to the lower energy exciton state. The theoretically predicted electronic spectra of compounds studied

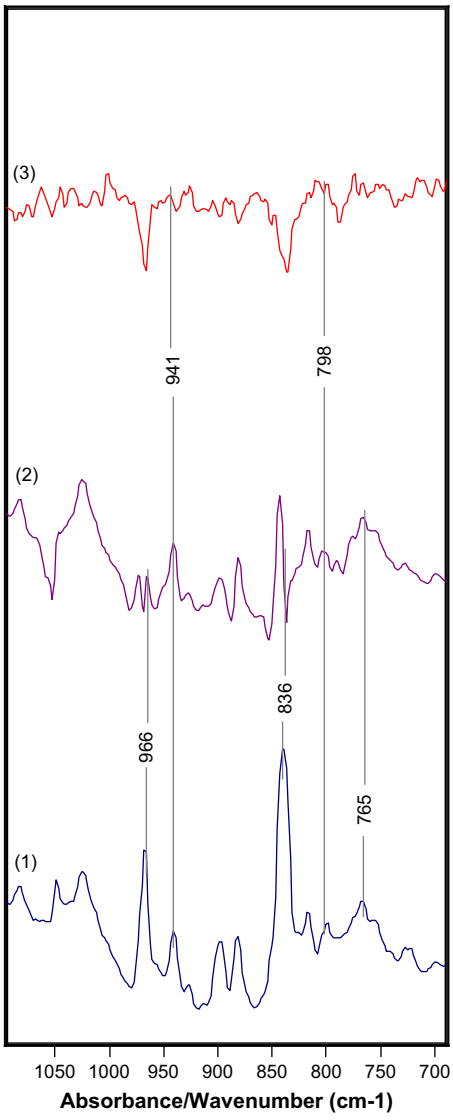

Fig. 3. Non-polarized IR (1) and reduced IR-LD (2) spectra of 1-methyl-4-[2-(4-hydroxyphenyl)ethenyl]pyridinium hydrogenphosphate after the elimination of the bands at 966 cm^{-1} (2) and 941 cm^{-1} (3).

show an excellent correlation with experimental data. In our case the CIS/6-311++G** method gives a $\Delta\lambda$ difference of 5 nm, while TDDFT calculations gave better values with difference less than 3 nm.

3.4. Calculated NLO properties

The calculated ground state dipole moment with the electron correlation methods (B3LYP) is 12.3052 Debye. As positively charged molecules, the compounds studied possess very large dipole moment. The polarity is noted as another important structural factor for upconversion [29] lasing. The calculated quadrupole moments in Debye-Å ($XX = 11.67_9$, $YY = -70.51_0$, $ZZ = -101.31_2$, $XY = -12.27_1$, $XZ = -0.00_2$, $YZ = -0.00_0$) and octapole moment in Debye-$Å^2$ ($XXX = 359.14_1$, $YYY = 2.51_3$, $ZZZ = 0.00_1$, $XYY = 3.87_9$, $XXY = 68.87_9$, $XXZ = 0.00_7$, $XZZ = 5.76_8$, $YZZ = -1.36_7$, $YYZ = -0.00_1$, $XYZ = -0.01_1$) are over 8.2 times larger than the corresponding ones of *p*-nitroaniline [32–34], independent of different symmetries of the molecules. The calculated hexadecapole moment (Debye-$Å^3$) shown as well a significant values then used reference material of $XXXX = -4463.29_3$, $YYYY = -510.83_9$, $ZZZZ = -108.07_0$, $XXXY = -569.56_2$, $XXXZ = -0.05_9$, $YYYX = -8.22_5$, $YYYZ = -0.00_1$, $ZZZX = 0.00_9$, $ZZZY = -0.00_1$, $XXYY = -1055.82_3$, $XXZZ = -1393.05_3$, $YYZZ = -132.94_1$, $XXYZ = 0.00_1$, $YYXZ = -0.00_7$ and $ZZXY = -14.29_2$, respectively.

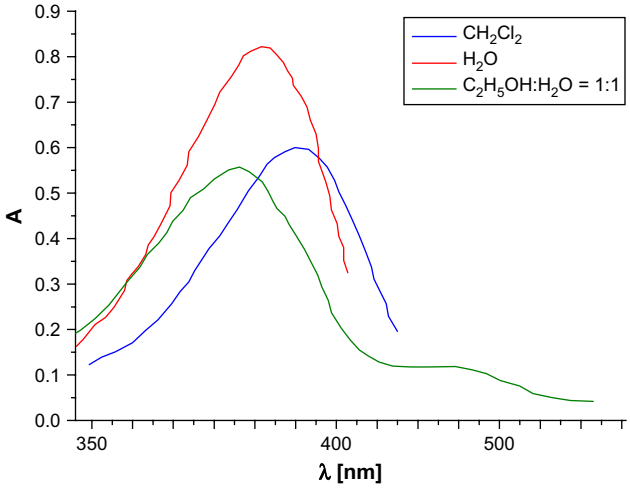

Fig. 4. UV–vis spectra of 1-methyl-4-[2-(4-hydroxyphenyl)ethenyl]pyridinium hydrogenphosphate in different media at a concentration of 2.5×10^{-5} M.

4. Conclusions

The 1-methyl-4-[2-(4-hydroxyphenyl)ethenyl]pyridinium salt of dihydrogenphosphate has been synthesized, and structurally elucidated by employing single crystal X-ray diffraction, linear-polarized solid-state IR spectroscopy, UV–vis spectroscopy, and TGA, DSC, DTA and MS methods. The compound crystallizes in the monoclinic $P2_1/c$ space group and exhibits a pseudo layer structure with molecules linked by strong OH···O–P intermolecular hydrogen bonds with a length of 2.597 Å. The dihydrogenphosphate anions form infinite chains through strong OH···O–P intermolecular hydrogen bonds with lengths of 2.630 Å. Similar to other merocyanine dyes a crystallographic disorder of the central C=C double bond is observed which reflects a deviation from a fully conjugated π system. Crystallographic data of

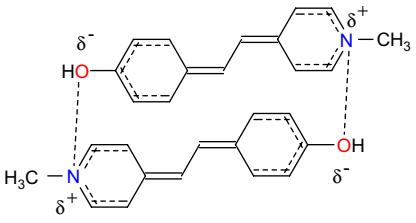

Scheme 4. H-aggregates in acetonitrile solvent.

the partial distortion of aromatic character are supported by the IR-LD spectroscopy in solid state. It is proved that in parallel with the aromatic IR characteristics of the in-plane and out-of-plane modes, low intensive bands typical for quinoide form of merocyanine dyes are observed. The UV-spectroscopic data in solution show the formation of classical H-aggregates in polar protic solvent mixture. The data in solutions with different polarity indicate a significant CT band shifting up to 70 nm, corresponding to a great molecular first hyperpolarizability value. The calculations of IR spectroscopic properties confirm the experimentally obtained data. The theoretically predicted NLO properties on molecular level and obtained value of β_{tot}, which is 8.2 times higher than the value of *p*-nitroaniline, a harismatic compound with experimentally confirmed NLO properties.

5. Supplementary materials

Crystallographic data for the structural analysis have been deposited with the Cambridge Crystallographic Data Centre, CCDC 651594. Copies of this information may be obtained from the Director, CCDC, 12 Union Road, Cambridge, CB2 1EZ, UK (fax: +44 1223 336 033; e-mail: deposit@ccdc.cam.ac.uk or http://www.ccdc.cam.ac.uk).

Acknowledgements

T.K. and M.S. wish to thank the DAAD for a grant within the priority program ''Stability Pact South-Eastern Europe'' and the Alexander von Humboldt Foundation. B.B.K. thanks the Alexander von Humboldt Foundation for the Fellowship.

References

[1] Marder SRJ, Perry W, Schaefer WP. Science 1989;245:626.
[2] Marder SR, Perry JW, Tiemann BG, Warsh RE, Schaefer WP. Chem Mater 1990;2:685.
[3] Ashwell GJ, Hargreaves RC, Baldwin CE, Bahra G, Brown CR. Nature 1992;357:6377.
[4] Lupo D, Prass W, Scheunemann U, Laschewsky A, Ringsdorf R, Ledoux IJ. J Opt Soc Am B 1988;5:300.
[5] Kolev TM, Yancheva DY, Stoyanov SI. Adv Funct Mater 2004;14:799.
[6] Kolev T, Wortmann R, Spiteller M, Sheldrick WS, Heller M. Acta Crystallogr 2004;E60:o1374.
[7] Kolev T, Wortmann R, Spiteller M, Sheldrick W, Mayer-Figge H. Acta Crystallogr 2005;E61:o1090.
[8] Kolev T, Stamboliyska B, Yancheva D. Chem Phys 2006;324:489.
[9] Sheldrick GM. SHELXTL, Release 5.03 for Siemens R3 crystallographic research system. Madison, USA: Siemens Analytical X-Ray Instruments, Inc.; 1995.
[10] Sheldrick GM. SHELXS97 and SHELXL97. Germany: University of Goettingen; 1997.
[11] Ivanova BB, Arnaudov MG, Bontchev PR. Spectrochim Acta 2004;60A(4):855.
[12] Ivanova BB, Tsalev DL, Arnaudov MG. Talanta 2006;69:822.
[13] Ivanova BB, Simeonov VD, Arnaudov MG, Tsalev DL. Spectrochim Acta 2007;67A:66.
[14] Ivanova BBJ. J Mol Struct 2006;782:122.
[15] Ivanova BB. Spectrochim Acta 2006;64A:931.
[16] Ivanova BB, Kolev T, Zareva S. Biopolymers 2006;82:587.
[17] Kolev Ts. Biopolymers 2006;83:39.
[18] Jordanov B, Schrader BJ. J Mol Struct 1995;347:389.
[19] Jordanov B, Nentchovska R, Schrader BJ. J Mol Struct 1993;297:2922.
[20] Michl J, Thulstrup EW. Spectroscopy with polarized light. Solute alignment by photoselection, in liquid crystals, polymers, and membranes. NY: VCH Publishers; 1986.
[21] Thulstrup EW, Eggers JH. Chem Phys Lett 1996;1:690.
[22] Frisch MJ, Trucks GW, Schlegel HB, Scuseria GE, Robb MA, Cheeseman JR, et al. Gaussian 98. Pittsburgh, PA: Gaussian, Inc.; 1998.
[23] Zhurko GA, Zhurko DA. ChemCraft: tool for treatment of chemical data, Lite version build 08 (freeware); 2005.
[24] Gruselle M, Malezieux B, Benard S, Train C, Guyard-Duhayon C, Gredin P, et al. Tetrahedron Asymmetry 2004;15:3103.
[25] Cariati E, Ugo R, Cariati F, Roberto D, Masciocchi N, Galli S, et al. Adv Mater 2001;13:1665.
[26] Tan X, Sun S, Yu W, Xing D, Wang Y, Qi C. Acta Crystallogr 2004;60E:o1054.
[27] Ren P, Qin J, Chen C, Zhang D, Hu HJ. J Chem Crystallogr 2004;34:291.
[28] Benard S, Yu P, Audiere JP, Riviere E, Clement R, Guilhem J, et al. J Am Chem Soc 2000;122:9444.
[29] Yan R, Qi F, Wen-Tao Y, Hong L, Yu-Peng T, Min-Hua J, et al. J Mater Chem 2000;10:2025.
[30] Harada J, Ogava K, Comoda SJ. J Am Chem Soc 1995;117:4476.
[31] Harada J, Ogava K, Comoda S. Acta Crystallogr 1997;B53:662.
[32] Jensen L, van Duijnen PTh. J Chem Phys 2005;123:074.
[33] Kimura T, Duan X-M, Kato M, Matsuda H, Fukuda T, Yamada S, et al. Macromol Chem Phys 1998;199:1193.
[34] Acebal P, Blaya S, Carretero L. J Phys B At Mol Opt Phys 2003;36:2445.